



HAL
open science

System with a nonlinear negative self-excitation

P. Půst Ladislav, Tondl Aleš

► **To cite this version:**

P. Půst Ladislav, Tondl Aleš. System with a nonlinear negative self-excitation. International Journal of Non-Linear Mechanics, 2008, 43 (6), pp.497. 10.1016/j.ijnonlinmec.2007.10.002 . hal-00501763

HAL Id: hal-00501763

<https://hal.science/hal-00501763>

Submitted on 12 Jul 2010

HAL is a multi-disciplinary open access archive for the deposit and dissemination of scientific research documents, whether they are published or not. The documents may come from teaching and research institutions in France or abroad, or from public or private research centers.

L'archive ouverte pluridisciplinaire **HAL**, est destinée au dépôt et à la diffusion de documents scientifiques de niveau recherche, publiés ou non, émanant des établissements d'enseignement et de recherche français ou étrangers, des laboratoires publics ou privés.

Author's Accepted Manuscript

System with a nonlinear negative self-excitation

Půst Ladislav, Tondl Aleš

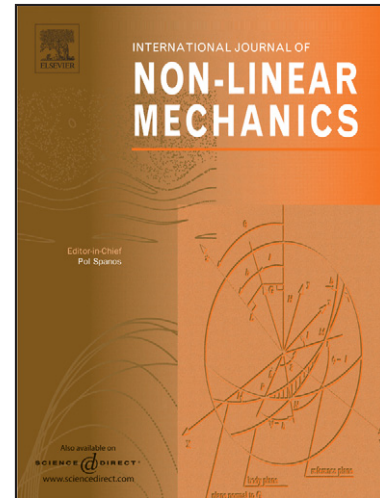
PII: S0020-7462(07)00199-0
DOI: doi:10.1016/j.ijnonlinmec.2007.10.002
Reference: NLM 1408

To appear in: *International Journal of Non-Linear Mechanics*

Received date: 22 August 2007
Accepted date: 3 October 2007

Cite this article as: Půst Ladislav and Tondl Aleš, System with a nonlinear negative self-excitation, *International Journal of Non-Linear Mechanics* (2007), doi:10.1016/j.ijnonlinmec.2007.10.002

This is a PDF file of an unedited manuscript that has been accepted for publication. As a service to our customers we are providing this early version of the manuscript. The manuscript will undergo copyediting, typesetting, and review of the resulting galley proof before it is published in its final citable form. Please note that during the production process errors may be discovered which could affect the content, and all legal disclaimers that apply to the journal pertain.



www.elsevier.com/locate/nlm

System with a Nonlinear Negative Self-excitation

Půst Ladislav

Institute of Thermomechanics, Academy of Sciences of the CR, 182 00 Prague 8, Czech Republic

Tondl Aleš

Zborovská 41, 150 00 Prague 5, Czech Republic

Abstract

A two-mass system is analyzed consisting of a self-excited basic system, which is mounted on a foundation subsystem consisting of a mass on a spring. The self-excitation is expressed in differential equations by a nonlinear term of the second power. The efficiency of the self-excited vibration suppressing of different positive damping components in both the subsystems is investigated by means of analytical and numerical solution. Phase plane trajectories gained by numerical solution show the distortion of pure harmonic forms of oscillations presumed in analytical solution. Ranges of system parameters in which the approximate bifurcation diagrams coincide with numerical results are ascertained.

Key words: nonlinear self-excitation, basic and foundation subsystems, effect of different damping components

1. Introduction

The prevailing part of self-excited systems analyzed up to now in literature belongs to the class of systems where the source of self-excitation is characterized by the negative linear damping component. But a negative nonlinear damping component can also exist. Although there exist an enormous amount of literature dealing with systems excited by the action of the negative linear damping component, the analysis of negative nonlinear damping components does practically not exist. From the theoretical point of view these systems can be represented by a broad class of systems.

In most cases the self-excited vibration represents an undesirable phenomenon, particularly in rotor-dynamics (see e.g. [1]-[5]) and it is a question how to suppress this vibration. For example how to use the passive means (e.g. using a tuned absorber or a foundation mass subsystems) and which character of additional passive damping would be most efficient in these subsystems. In [6] it is shown that for systems where the source of self-excitation is due to the action of negative linear damping the above mentioned additional subsystems using linear positive damping can even fully suppress self-excited vibration when certain conditions are met. This is not the case when the basic self-excited system is governed by differential equations where the self-excitation is expressed by nonlinear terms. An example thereof is the mathematical model of a system excited by vortex shedding where the self-excitation is described by the nonlinear term of zero power (see [6], Chapter 12). For this system to add a subsystem of a tuned absorber or a foundation subsystem with linear damping does not lead to full suppressing the self-excited vibration of this kind (see also in [6]).

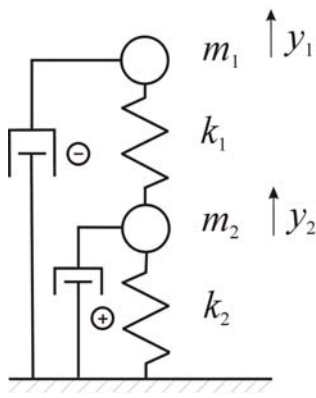
This presented analysis is a contribution to the case where the source of self-excitation is due to the negative nonlinear damping characterized by the term of second power (see also [12]). As a means of vibration suppression a foundation subsystem is considered.

This model represents a more intensive self-excitation than that expressed by the negative linear damping. It will be shown the existence possibility of more steady state solutions of the differential equations of motion.

2. Differential equations of motion

Let us consider a one-mass system which is self-excited by a nonlinear negative damping component expressed by the product of the absolute value of the mass deflection and its velocity ($|y_1| \dot{y}_1$). Besides the negative nonlinear damping a positive progressive damping component is acting expressed by the product of the square of the mass deflection and velocity.

Both the above-mentioned damping components are proportional to the square of the flow velocity U . Also a positive linear viscous component of the mass m_1 motion is considered in



order to get a more general idea on the effect of different damping components. This basic system characterized by mass m_1 on the spring having stiffness k_1 is attached to the foundation subsystem characterized by mass m_2 suspended on a spring having stiffness k_2 , (see Fig. 1). The foundation mass motion is damped by two positive damping components – viscous linear and nonlinear characterized by the product of the absolute value of the deflection $|y_2|$ and its velocity \dot{y}_2 . The system is governed by the following equations:

Fig. 1

$$m_1 \ddot{y}_1 + k_1 (y_1 - y_2) + b_1 \dot{y}_1 - U^2 (b |y_1| - d y_1^2) \dot{y}_1 = 0, \quad (2.1)$$

$$m_2 \ddot{y}_2 - k_1 (y_1 - y_2) + k_2 y_2 + b_2 \dot{y}_2 + b_0 |y_2| \dot{y}_2 = 0.$$

Denoting $\omega_1^2 = k_1 / m_1$ and using time transformation $\omega_1 t = \tau$ and relative deflections $y_j / y_0 = u_j$ ($j = 1, 2$) equations (2.1) can be transformed into the dimensionless form

$$u_1'' + u_1 - u_2 + \kappa_1 u_1' - V^2 (\beta |u_1| - \delta u_1^2) u_1' = 0, \quad (2.2)$$

$$u_2'' + q^2 u_2 - M (u_1 - u_2) + \kappa_2 u_2' + \vartheta |u_2| u_2' = 0,$$

where

$$\frac{b_1}{m_1 \omega_1} = \kappa_1, \quad V = \frac{U}{U_0}, \quad \frac{b U_0^2 y_0}{m_1 \omega_1} = \beta, \quad \frac{d y_0^2 U_0^2}{m_1 \omega_1} = \delta, \quad M = \frac{m_1}{m_2}, \quad \frac{k_2}{m_2 \omega_1^2} = q^2,$$

$$\frac{b_2}{m_2 \omega_1} = \kappa_2, \quad \vartheta = \frac{b_0 y_0}{m_2 \omega_1} \quad \text{and } U_0 \text{ and } y_0 \text{ are chosen values.}$$

Let us start with the analysis of the basic system which is governed by the following equations:

$$u_1'' + u_1 + \kappa_1 u_1' - V^2 (\beta |u_1| - \delta u_1^2) u_1' = 0. \quad (2.3)$$

Seeking the solution in the form

$$u_1 = A \cos \Omega \tau \quad (2.4)$$

and using the method of harmonic balance the following algebraic equations are obtained:

$$A(1 - \Omega^2) = 0, \quad (2.5)$$

$$\left[\kappa_1 - V^2 \left(\frac{4}{3\pi} \beta A - \frac{1}{4} \delta A^2 \right) \right] \Omega A = 0.$$

From the first one it follows that $\Omega = 1$; then the second equation gets the form

$$A^2 - 4 \frac{\bar{\beta}}{\delta} A + 4 \frac{\kappa_1}{\delta V^2} = 0$$

where

$$\bar{\beta} = \frac{4}{3\pi} \beta. \quad (2.6)$$

For $\kappa_1 = 0$

$$A = 4 \frac{\bar{\beta}}{\delta} \quad (2.7)$$

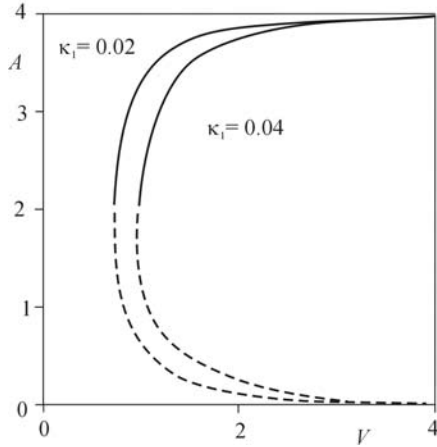


Fig. 2

is obtained, i.e. amplitude A is independent on V . Fig. 2 shows amplitude A in dependence on V for two alternatives (a) $\bar{\beta} = \delta = \kappa_1 = 0.04$. ; (b) $\bar{\beta} = \delta$, $\kappa_1 = 0.02$.

For alternative (a) the curve has two branches: with higher values of A (solid line) and lower values of A (dash line) corresponding to stable and unstable limit cycles in the phase plane (u_1, u_1') correspond.

Let us go back to the system with 2 DOF. Supposing that all the damping coefficients are small system (2.2) can be transformed into the quasi-normal form using transformation

$$u_1 = x_1 + x_2, \quad u_2 = a_1 x_1 + a_2 x_2 \quad (2.8)$$

where

$$a_1 = \frac{M}{q^2 + M - \Omega_1^2}, \quad a_2 = \frac{M}{q^2 + M - \Omega_2^2}$$

and Ω_1, Ω_2 are the roots of the characteristic equation of the abbreviated system. The following relations are valid for a_1, a_2 :

$$a_1 > 0, \quad a_2 < 0. \quad (2.9)$$

In this way the differential equations in the quasi-normal form read:

$$\begin{aligned} x_1'' + \Omega_1^2 x_1 + \frac{a_2}{a_1 - a_2} \left\{ -\kappa_1 + V^2 \left[\beta |x_1 + x_2| - \delta (x_1 + x_2)^2 \right] \right\} (x_1' + x_2') + \\ + \frac{1}{a_1 - a_2} \left[\kappa_2 + \mathcal{G} |a_1 x_1 + a_2 x_2| \right] (a_1 x_1' + a_2 x_2') = 0, \\ x_2'' + \Omega_2^2 x_2 + \frac{a_1}{a_1 - a_2} \left\{ \kappa_1 - V^2 \left[\beta |x_1 + x_2| - \delta (x_1 + x_2)^2 \right] \right\} (x_1' + x_2') - \\ - \frac{1}{a_1 - a_2} \left[\kappa_2 + \mathcal{G} |a_1 x_1 + a_2 x_2| \right] (a_1 x_1' + a_2 x_2') = 0. \end{aligned} \quad (2.10)$$

Now we shall seek the single-frequency vibration with the first and second vibration modes. The steady state vibration with the first mode can be approximated in the form:

$$x_1 = X_1 \cos \tau, \quad x_2 = 0. \quad (2.11)$$

Using the harmonic balance method the following algebraic equations are obtained:

$$\begin{aligned} (\Omega_1^2 - \Omega^2) X_1 = 0, \\ -a_2 \left[\kappa_1 - V^2 \left(\bar{\beta} X_1 - \frac{\delta}{4} X_1^2 \right) \right] \Omega X_1 + (\kappa_2 + \bar{\mathcal{G}} a_1 X_1) a_1 \Omega X_1 = 0 \end{aligned} \quad (2.12)$$

where

$$\bar{\mathcal{G}} = \frac{4}{3\pi} \mathcal{G}, \quad \bar{\beta} = \frac{4}{3\pi} \beta, \quad \left(\text{considering that } \frac{\Omega}{\pi} \int_0^{2\pi/\Omega} |\cos \Omega t| \sin^2 \Omega \tau d\tau = \frac{4}{3\pi} \right).$$

From the first equation it follows:

$$\Omega = \Omega_1$$

and from the second one equation $X_1 = 0$ or

$$\frac{\delta}{4} V^2 X_1^2 - \left(\bar{\beta} V^2 + \frac{a_1^2}{a_2} \bar{\mathcal{G}} \right) X_1 + \kappa_1 - \frac{a_1}{a_2} \kappa_2 = 0. \quad (2.13)$$

From this amplitude X_1 as a function of V can be obtained or, from the inversion function $V(X_1)$ using equation

$$V^2 = \left[\kappa_1 - \frac{a_1}{a_2} (\kappa_2 + \bar{g} a_1 X_1) \right] / \left(\bar{\beta} X_1 - \frac{\delta}{4} X_1^2 \right). \quad (2.14)$$

For the alternative $\kappa_1 = \kappa_2 = 0$ amplitude X_1 can be determined from the equation

$$X_1 = 4 \left(\frac{\bar{\beta}}{\delta} + \frac{\bar{g}}{\delta} \frac{a_1^2}{a_2 V^2} \right). \quad (2.15)$$

Considering that $a_2 < 0$ we can see that X_1 has sense when $V > V_{c1}$ where V_{c1} is the critical value of the relative flow velocity (for the first vibration mode) given by the equation:

$$V_{c1}^2 = -\frac{a_1^2 \bar{g}}{a_2 \bar{\beta}}. \quad (2.16)$$

Using similar approach for the second vibration mode and applying the approximation

$$x_1 = 0, \quad x_2 = X_2 \cos \Omega \tau \quad (2.17)$$

the following equations are obtained:

$$\Omega = \Omega_2, \quad (2.18)$$

$$\frac{\delta}{4} V^2 X_2^2 - \left(\bar{\beta} V^2 + \frac{a_2 |a_2| \bar{g}}{a_1} \right) X_2 + \kappa_1 - \frac{a_2}{a_1} \kappa_2 = 0 \quad (2.19)$$

Again amplitude X_2 as a function of V can be determined either from the quadratic equation for X_2 or from the inversion function $V(X_2)$ that can be determined using equation:

$$V^2 = \left[\kappa_1 - \frac{a_2}{a_1} (\kappa_2 - a_2 \bar{g} X_2) \right] / \left(\bar{\beta} X_2 - \frac{\delta}{4} X_2^2 \right). \quad (2.20)$$

For the alternative of zero value of the coefficients of linear positive damping coefficients, i.g. for $\kappa_1 = \kappa_2 = 0$, the following relations are valid:

$$X_2 = 4 \left(\frac{\bar{\beta}}{\delta} - \frac{\bar{g}}{\delta} \frac{a_2^2}{a_1 V^2} \right), \quad (2.21)$$

$$V_{c2}^2 = \frac{\bar{g}}{\bar{\beta}} \frac{a_2^2}{a_1}. \quad (2.21a)$$

In case when $\kappa_1 = \kappa_2 = 0$ the mentioned critical values V_{c1} , V_{c2} mean that for $V > V_{c1}$ self-excited vibration with the first vibration mode occurs and the equilibrium position is unstable to this vibration mode. A similar situation is when $V > V_{c2}$. For $V_{c1} < V_{c2}$ the equilibrium position is absolutely stable for $V < V_{c1}$. When V exceeds the both critical values then three

different vibrations can exist: two single-frequency vibrations and one two-frequency vibration. There can exist three domains of attracting leading to different types of vibration. This problem is not treated in this contribution.

For illustration the dependence of X_1 , X_2 on V is shown in Fig. 3 the case $q^2 = M = 0.5$ and for three alternatives of damping coefficients:

$$\begin{aligned} /a/ \quad & \bar{\beta} = \delta = 2\kappa_1 = 2\kappa_2 = 0.04, \quad \bar{\varrho} = 0; \\ /b/ \quad & \bar{\beta} = \delta = \bar{\varrho} = 0.04, \quad \kappa_1 = \kappa_2 = 0; \\ /c/ \quad & \bar{\beta} = \delta = \bar{\varrho} = 2\kappa_1 = 2\kappa_2 = 0.04; \end{aligned} \quad (2.22)$$

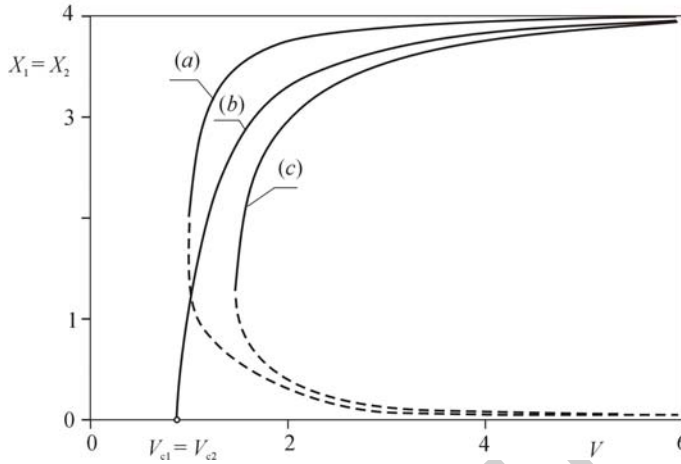


Fig. 3

stable because the corresponding equations for small disturbances are linear with positive damping.

In case when either $\kappa_1 \neq 0$, or $\kappa_2 \neq 0$ or even both the coefficients κ_1 , κ_2 differ from zero value then the trivial solution (i.e. equilibrium position) is stable but not absolutely stable in the whole range of V values. From a certain value of V up to the higher values there exist locally oscillatory solutions besides the locally stable equilibrium position. Let us denote this value of V as $V_{1\min}$ or $V_{2\min}$ according to whether it corresponds to the oscillatory solution with lower or higher vibration mode. These values can be determined from the equations for determining amplitudes X or X resp. from the condition that the roots of the equation expressing X_1 or X_2 merge into one. This can be symbolically expressed by equation:

$$Q_2(V^2)X_j^2 - Q_1(V^2)X_j + Q_0 = 0 \quad (j=1, 2) \quad (2.23)$$

and which is a biquadrate equation for V where Q_2 , Q_1 are the functions of V^2 . Then the above mentioned condition reads:

$$[Q_1(V^2)]^2 - 4Q_2(V^2)Q_0 = 0 \quad (2.24)$$

The minimum value of V determines $V_{j\min}$ ($j=1, 2$).

because for $q^2 = M = 0.5$ $a_1 = |a_2|$ the dependences $X_1(V)$, $X_2(V)$ are identical. The parts where the corresponding solutions are unstable are marked by dash lines. For alternatives /a/ and /c/ the trivial solution is stable in the whole range of V ; for alternative /b/ only for $V < V_c$. For alternatives (a) and (c) the equilibrium position corresponding to trivial solutions of differential equations of motion is

$$\text{For } V_{1\min} : \quad Q_2(V^2) = \frac{\delta}{4} V^2, \quad Q_1(V^2) = \left(\bar{\beta} V^2 + \frac{a_1^2}{a_2} \bar{g} \right), \quad Q_0 = \kappa_1 - \frac{a_1}{a_2} \kappa_2 ;$$

$$\text{For } V_{2\min} : \quad Q_2(V) = \frac{\delta}{4} V^2, \quad Q_1(V^2) = \left(\bar{\beta} V^2 + \frac{a_2 |a_2|}{a_1} \bar{g} \right), \quad Q_0 = \kappa_1 - \frac{a_2}{a_1} \kappa_2 .$$

For further illustration diagrams of $X_1(V)$, $X_2(V)$ are shown in Figs. 4 and 5 both for $\kappa_1 = \kappa_2 = 0$ and $\bar{\beta} = \delta = \bar{g} = 0.04$. The alternative for $M = q^2 = 1$ is shown in Fig. 4 and the

Fig. 5

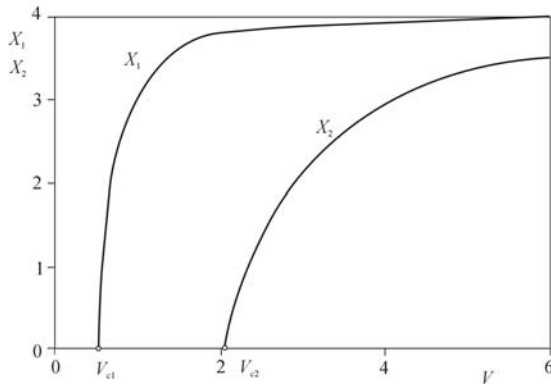


Fig. 4

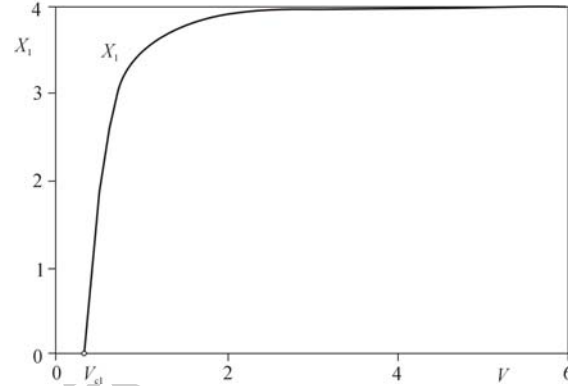


Fig. 5

alternative for $M = 5$, $q = 1$ in Fig. 5. In the latter alternative only $X_1(V)$ is presented because $V_{c2} = 6.334$ is higher than 6. We can see that for higher values of M the initiation of self-excited vibration when the higher mode is really shifted to higher values of the relative flow velocity V .

V_c and V_{\min} values determine the coordinates of V for bifurcation points of different kind. These bifurcations corresponding to V_c coordinates are similar to Hopf bifurcation and these corresponding to V_{\min} are similar to saddle-node bifurcation. For the alternatives when $V > V_{\min}$ there exist locally stable trivial solution and also one or two oscillatory solutions corresponding to the first or second vibration mode or even oscillatory solution with both vibration modes. To determine the domains of attraction corresponding to different steady state solutions would need special methods.

3. Numerical solution

The equations (2.2) contain eight different coefficients κ_1 , V , β , δ , q , M , κ_2 , g which affect the dynamic behavior of the whole 2 DOF systems. The general qualitative analysis of the system properties carried out in the previous chapter was orientated on the analytical approximate solution. In this chapter, the numerical solution of the basic equations (2. 2) is presented using the set program in Turbo Pascal elaborated together with F. Peterka ([7]-[10]) and using Runge-Kutta integration algorithm. The influence of individual parameters are studied quantitatively. The following figures plot the maximum displacements $u_{1\max}$ and $u_{2\max}$ versus dimensionless flow velocity $V = U/U_0$ for very slowly increasing or decreasing velocity in the range $V \in (1, 6)$. The velocity change near critical point was lower than $1 \cdot 10^{-6} V / \text{period}$, so that the records are quasi-stationary.

Records of bifurcation diagrams are completed by records of time history and of phase plane trajectories $u_1(\tau)$, $u_1'(\tau)$ and $u_2(\tau)$, $u_2'(\tau)$ for selected values of dimensionless flow velocity V . These diagrams show the real course of the motion and serve as a verification of correctness of assumption of harmonic form of oscillations.

There exists only trivial solution ($u_{1\max} = 0$, $u_{2\max} = 0$) when increasing velocity V . This trivial solution is stable if at least one of κ_1 or κ_2 is positive. In the critical case, when $\kappa_1 = \kappa_2 = 0$, the stability of the solution depends according to Ljapunov [11] on the nonlinear function and can be either stable (e.g. for large \mathcal{G}) or unstable (for small \mathcal{G}). Nontrivial oscillations can be initiated only at high initial conditions and at higher V . Therefore the records of nontrivial solutions are realized at decreasing velocities V and at initial conditions $V \cong 6$, $u_1(0) = 3$, $u_2(0) = 3$, $u_1'(0) = 1$, $u_2'(0) = 1$. For the prescribed system parameters, the solution with all other initial values sufficiently near to the mentioned ones pass over to the same stationary motion.

As an example of influence of damping parameter κ_1 are the bifurcation diagrams in Fig. 6. The first curve $\kappa_1 = 0$ and $\kappa_2 = 0$ corresponds to the critical case b) in (Fig. 3). The other parameters are: $\bar{\beta} = \delta = \bar{\mathcal{G}} = 0.04$, $\beta = 3\pi\bar{\beta}/4 = \mathcal{G} = 3\pi\bar{\mathcal{G}}/4 = 0.9425$, $q^2 = M = 0.5$.

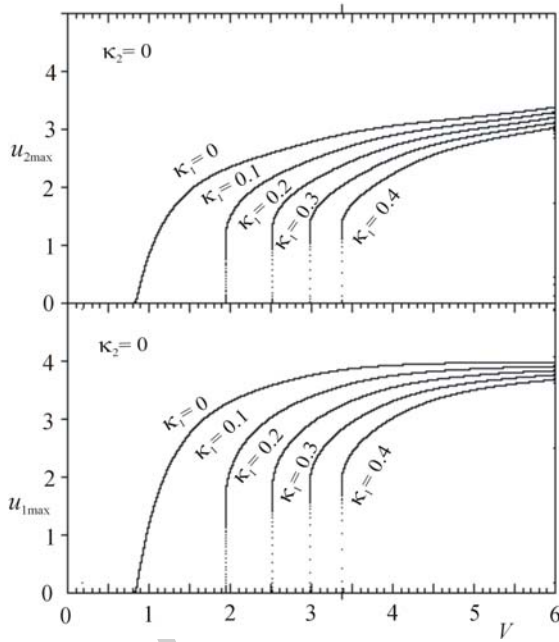


Fig. 6

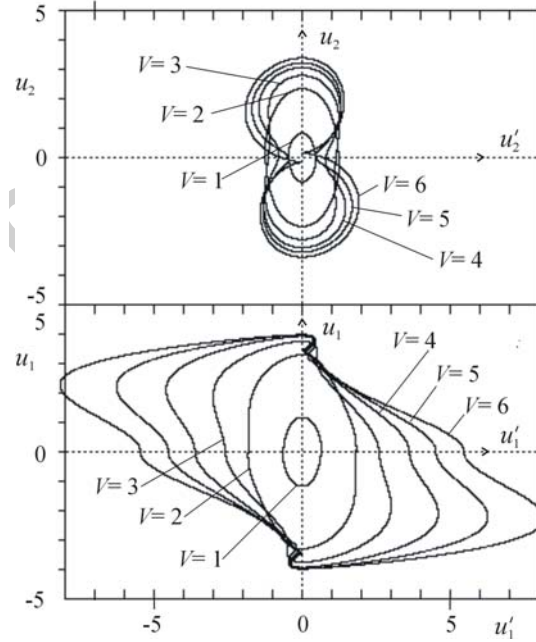


Fig. 7

The upper half of Fig. 6 shows the bifurcation diagram $u_{2\max}, V$, the bottom half those for $u_{1\max}, V$, where the dimensionless velocity parameter $V \in (0, 6)$. The other curves in Fig. 6 describe the curves $u_{2\max}, V$ and $u_{1\max}, V$ for increasing damping parameter κ_1 , step 0.1. Step 0.1 is dimensionless, as the damping parameter is also dimensionless (see eq. 2.2).

The vertical lines indicate the jumps to zero values $u_1 = u_2 = 0$ (trivial solution) at $V = V_{\text{crit}}$. The bifurcations points where these jumps downwards begin are always near to the value $u_{1\max} \cong 2$, $u_{2\max} \cong 1.4$. The ratio $u_{2\max} / u_{1\max} = 0.7$ is typical for first mode of oscillations but it changes with higher velocity V .

In order to ascertain the real property of the system described by e.g. (2.2), the phase plane trajectories for different velocities $V=1; 2; 3; 4; 5$ and 6 are recorded in Fig. 7. Ellipse forms corresponding to nearly harmonic motion (e.g. 2.4) exist only for $V=1$ and 2 , the distortion of curves for greater V indicates the presence of higher harmonic components.

This distortion, which can be explained by the strong nonlinear absolute values in (2.2), is clearly shown in time history of motion $u_1(\tau)$ and $u_2(\tau)$ in Fig. 8 at $V=6$ and particularly in velocities records $u_1'(\tau)$ and $u_2'(\tau)$ (second and fourth lines). In spite of the very marked peaks in the course of velocity u_1' , the motion is continuous without any non-smooth phenomena, as seen from the zoom Fig. 9. It is caused by the continuous functions on the right sides of eq. (2.2), which are only weakly non-smooth due to multiplication of absolute values by smooth functions u_1' and u_2' .

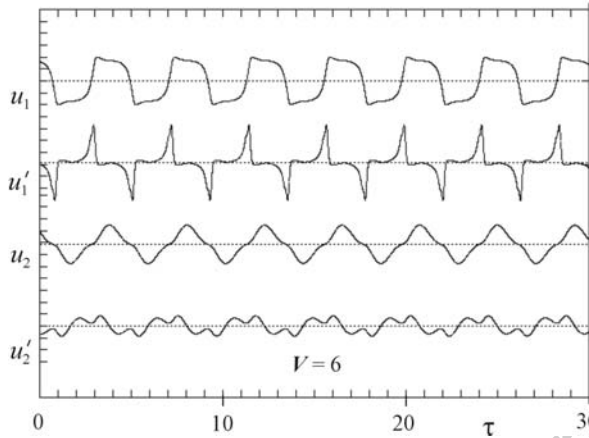


Fig. 8

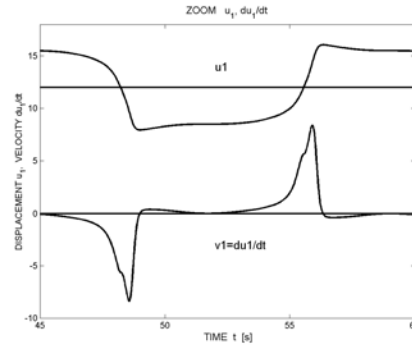


Fig. 9

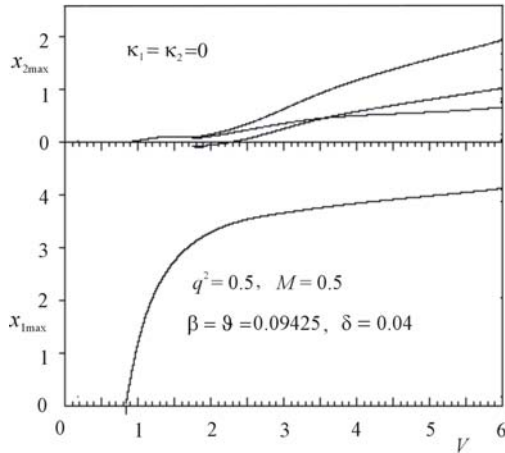


Fig. 10

Figures 6 -9 show that the assumption of harmonic solution (2.4) is quite convenient for small overcritical velocities near bifurcation point. The influence of break in absolute value is amplified by the large coefficients at nonlinear terms in eq. (2.2). In comparison to the coefficient 1 and κ_1 in linear part at u_1 and u_1' , the negative damping coefficient $V^2\beta$ grows quadratically with velocity V and at $V=6$ reaches for given example the value 3.39, indicating that the motion at these velocities is near to the relaxation oscillations. However, the range of V for roughly harmonic oscillations increases with lowering the parameters β, δ and ϱ of nonlinear terms.

Let us have a look now on the solution in quasi-normal form after transformation (2.8). Plots of maximal amplitudes $x_{1\max}$ and $x_{2\max}$ versus velocity V are shown in Fig. 10. It can be seen that for the low velocity range $V \in (V_{\text{crit}}, 2)$ the system oscillates mostly in the first mode, but for higher V the second mode component increases and reaches 46% of the first mode component at $V=6$. Unlike the plot $x_{1\max}, V$, the plot $x_{2\max}, V$ contains three curves indicating

that the motion $x_2(\tau)$ has three different maximum values. This property can be seen also from the upper half of Fig. 11, where the phase plane trajectory $x_2(\tau), x_2'(\tau)$ at $V=6$ has three loops. The corresponding curves $x_2(\tau), x_2'(\tau)$ at $V=6$ (bottom of Fig. 11) have

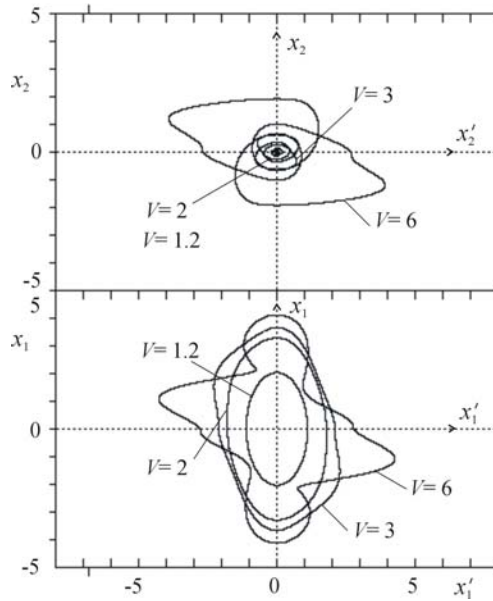


Fig. 11

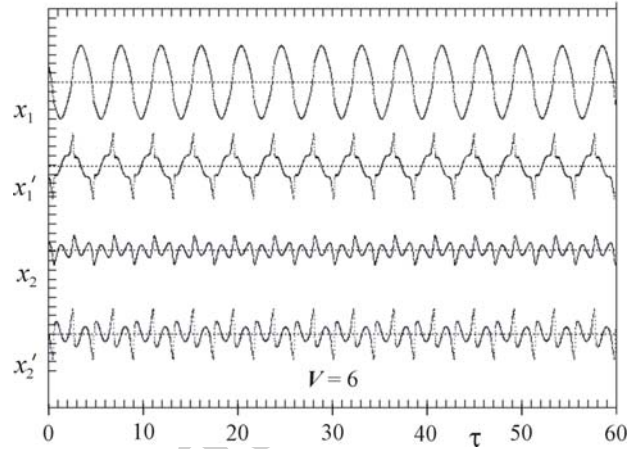


Fig. 12

very complicated forms, too. Harmonic oscillations and separation of modes can be therefore supposed only for small overcritical velocities $V \in (V_{\text{crit}}, 2)$. Examples of time history records $x_1(\tau), \dots, x_2'(\tau)$ in Fig. 12 present the system oscillations at $V=6$. The peaks in velocity curves $x_1'(\tau)$ and $x_2'(\tau)$ arise in the times when $x_1=0$, that is when the breaks of absolute value of x_1 occur. It is evident that the great distortion of motions x_1 and x_2 is caused both by the absolute value function and by the high values of coefficients at nonlinear terms.

The calculations of system oscillations for other values of parameters $\kappa_1, \kappa_2, \beta, \delta, \vartheta, q$ and M give qualitatively the same results.

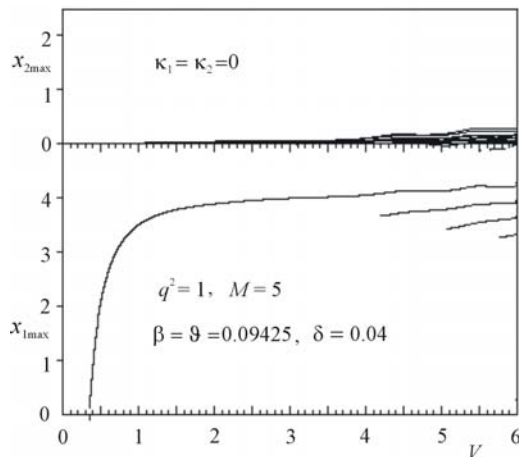


Fig. 13

Let us present only one example with the higher values of mass ratio $M = m_1/m_2 = 5$ and frequency ratio $q^2 = k_2/(m_2 \omega_1^2) = 1$ (see also Fig. 5). The modal bifurcation diagrams $x_{1\text{max}}, V$ and $x_{2\text{max}}, V$ in Fig. 13 are qualitatively similar to those of Fig. 10. The higher components in $x_{2\text{max}}, V$ are suppressed, but some new harmonic components occur in $x_{1\text{max}}, V$.

Conclusion

The new model of a self-excited 2DOF system with nonlinear excitation was solved analytically by the first approximation method (under the assumption of single-frequency vibration) and numerically by the direct solution of differential equations.

The comparison of both results enables to ascertain ranges of parameter values in which the single-frequency vibration with the first vibration mode occurs and the first approximation gives sufficient exact results and the motion is near to the harmonic one. This is valid for smaller values of flow velocity V . For higher values of flow velocity far from the critical one, the vibration with both mode components as well as with higher harmonics are initiated.

The main distortion of roughly harmonic course of oscillation is caused by the nonlinear non-smooth functions $|y_1|\dot{y}_1$ or $|y_2|\dot{y}_2$, particularly at higher coefficients at nonlinear terms.

The analysis results show that for systems with nonlinear self-excitation several steady state solutions can exist. The stable equilibrium position need not mean that the system is safe for self-excited vibration. Some disturbances can lead to violent vibration. This means that the stability investigations where in the model all forces are expressed only by linear terms does not always guarantee the save run of the machine or device.

Acknowledgement

This work was supported by the Grant Agency of the Czech Republic, project No.101/06/1787.

References

1. Muszynska, A., 'Whirl and Whip-Rotor/Bearing Stability Problems', *J. of Sound and Vibration* **110**(3), 1986, pp. 443-462
2. Taura H., Tanaka M., 'Self-excited vibration of elastic rotors in tilting pad journal bearings', in Proc. Eighth Int. Conf. On Vibrations in Rotating Machinery, IMechE Conference Transaction 2004-2, pp.35-43
3. Pan C.,H.,T., Kim D., Bryant M.,D., 'Use of Rotating Coordinates in Stability Analysis: Compilation of Numerical Result', in Proc.3rd ISCORMA, A. Carlisle Printers, NV 89502, pp. 458-467
4. Dimofte F., et al., 'Investigation of the Stability of a Rotor By Oil Journal Wave Bearing', in CD-ROM Proc. 7th Intern. Conference on Rotor Dynamics, TU Vienna, 2006, Paper ID-147
5. Czolczynski K., *Rotordynamics of Gas-lubricated Journal Bearing System*, Springer Verlag, New York, Inc., 1999
6. Tondl, A., *Quenching of Self-Excited Vibrations*, Academia, Prague in co-edition with Elsevier, Amsterdam, 1991.
7. Púst, L. and Peterka, F., 'Impact Oscillator with Hertz's Model of Contact', *Meccanica* **38**, 10, 2003, 99-114.
8. Púst, L. and Peterka, F., 'Impact System with Hertz Contact', in *Colloquium Dynamics of Machines 2001*, Institute of Thermomechanics ASCR, Prague 2001 pp. 167-174.
9. Púst, L., 'Improvement of Dynamic Absorber by Means of weak Stops', *Acta Technica CSAV* **48**, 2003, 273-299.
10. Peterka, F., 'Impact Oscillator, (Chapter 5), Impacts and Dry Friction, (Chapter 14)', in *Applied Nonlinear Dynamics and Chaos of Mechanical Systems with Discontinuities*, Editors: Marian Wiercigroch and Bram de Kraker, World Scientific Series on Nonlinear Sciences, Singapore, 2000.
11. Minorsky, N., *Nonlinear Oscillations*, D. Van Nostrand Company, Inc. New York, 1962.
12. Tondl, A., 'Effect of different alternatives of self-excitation and damping on the vibration quenching', in ROM Procc. *Engineering Mechanics 2006*, Svratka, UTAM ASCR, paper 199, 2006

- Fig. 1 Scheme of the system
- Fig. 2 Vibration amplitude A of the basic system in dependence on the relative flow velocity V for $\kappa_1 = 0.02$ and 0.04
- Fig. 3 Vibration amplitudes X_1, X_2 in dependence on flow velocity V for the following parameter values: $M = q^2 = 0.5$, and for three alternative of damping coefficients:
- (a) $\bar{\beta} = \delta = 2\kappa_1 = 2\kappa_2 = 0.04, \vartheta = 0$;
 - (b) $\bar{\beta} = \delta = \bar{\vartheta} = 0.04, \kappa_1 = \kappa_2 = 0$;
 - (c) $\bar{\beta} = \delta = \bar{\vartheta} = 2\kappa_1 = 2\kappa_2 = 0.04$;
- Fig. 4 Diagrams of $X_1(V), X_2(V)$ for $M = q = 1$ and $\kappa_1 = \kappa_2 = 0, \bar{\beta} = \delta = \bar{\vartheta} = 0.04$
- Fig. 5 Diagram of $X_1(V)$ for $M = 5, q = 1$ and the same damping coefficients as in Fig. 4.
- Fig. 6 Influence of damping parameter κ_1 on bifurcation diagrams $u_{1\max}, V$ and $u_{2\max}, V$
- Fig. 7 Phase plane trajectories u_2, u_2' and u_1, u_1' for different velocities V
- Fig. 8 Time history of motion $u_1(\tau), u_1'(\tau), u_2(\tau), u_2'(\tau)$ for flow velocity $V = 6$
- Fig. 9 Zoom diagram $u_1(\tau), u_1'(\tau)$
- Fig. 10 Bifurcation diagram of quasi-normal forms $x_{2\max}, V$ and $x_{1\max}, V$ for critical case $\kappa_1 = 0, \kappa_2 = 0$
- Fig. 11 Phase plane trajectories of quasi-normal solution x_2, x_2' and x_1, x_1' for different velocities V
- Fig. 12 Time history of quasi-normal oscillations, $x_1(\tau), x_1'(\tau), x_2(\tau), x_2'(\tau)$ for flow velocity $V = 6$
- Fig. 13 Bifurcation diagram of quasi-normal forms $x_{2\max}, V$ and $x_{1\max}, V$ for critical case $\kappa_1 = 0, \kappa_2 = 0$ and for $q^2 = 1, M = 5$